

GOA-1 regulates spermathecal transits

Fereshteh Sadeghian¹, Virginie Sjoelund², Erin J. Cram^{3§}

Abstract

G protein signaling regulates Ca^{2+} dynamics and contractility in the <u>C. elegans</u> spermatheca. G protein-coupled receptors activate heterotrimeric G proteins, triggering downstream cascades, including the Gαs-mediated activation of adenylyl cyclase and subsequent Protein Kinase A (PKA) activation. Our previous work identified <u>GSA-1</u>/Gαs and PKA as key modulators of Ca^{2+} oscillations and tissue contractility in the <u>C. elegans</u> spermatheca. In this study, we show that the inhibitory Gαi/o subunit <u>GOA-1</u> regulates spermathecal transit. We employed TurboID proximity labeling and mass spectrometry to identify 16 candidate interactors of <u>GOA-1</u>. Depletion of these candidates by RNAi did not yield overt spermathecal transit defects.

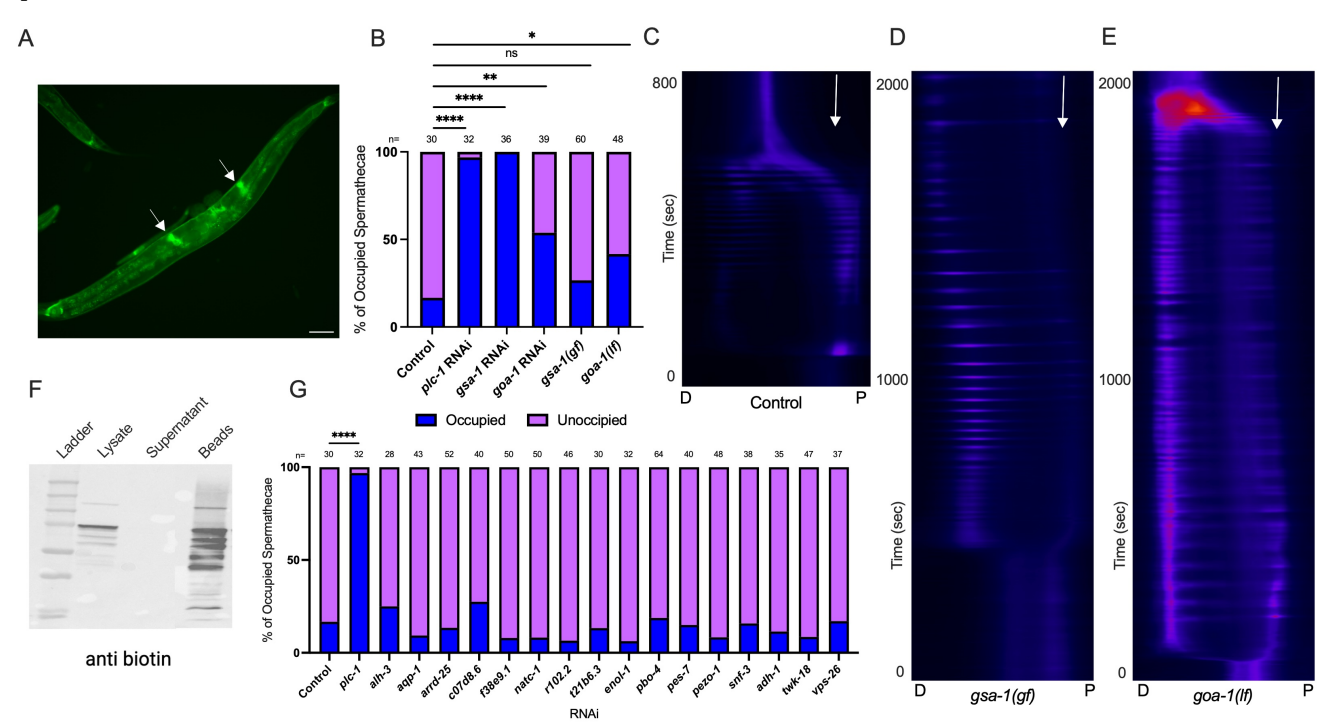


Figure 1. GOA-1 regulates transit of oocytes through the spermatheca:

A) GOA-1::GFP expression in the hermaphrodite *C. elegans*. Arrows indicate spermathecal expression (scale bar 100 μm). **B)** Spermathecal occupancy assay of *fln-1p*::GCaMP expressing animals grown on negative control (n=30), positive control *plc-1* RNAi (n=32), *gsa-1* RNAi (n=36), *goa-1* RNAi (n=39), *gsa-1(gf)* (n=60), and *goa-1(lf)* (n=48). C-E) Kymograms of Ca²⁺ transients in *fln-1p*::GCaMP expressing animals are shown for control (C), *gsa-1(gf)* (D) and *goa-1(lf)* (E) conditions. In D and E, the embryo fails to exit the spermatheca. In *gsa-1(gf)* time lapse movies 24% (n=17), and in *goa-1(lf)*, 53% (n=13) of the embryos failed to exit. The x axis indicates the spatial dimension from distal (D) to proximal (P) and the Y axis indicates the timepoint (s) in the transit. Arrows indicate the position of the spermathecauterine valve. **F)** Western blot detection of biotinylated proteins in the GOA-1::TurboID samples using an anti-biotin antibody. **G)** Spermathecal occupancy assay of *fln-1p*::GCaMP expressing animals grown on negative control, *plc-1* RNAi, and 16 TurboID targets (n=28-64). Spermathecae were scored for the presence or absence of an embryo (occupied or unoccupied) in the spermatheca. Fisher's exact test (with Benjamini-Hochberg correction) was used for the statistical analysis. Stars designate statistical significance (***** p<0.0001, **** p<0.005, *** p<0.01, ** p<0.05).

Description

¹Bioengineering, Northeastern University, Boston, MA

²Northeastern University, Boston, MA

³Biology, Northeastern University, Boston, MA

[§]To whom correspondence should be addressed: e.cram@northeastern.edu



Heterotrimeric G proteins are composed of an alpha (α), and a beta (β) gamma (γ) subunit, which, when activated by an upstream G protein-coupled receptor (GPCR) or G protein regulator (GPR), dissociate and independently trigger signaling cascades (Jastrzebska, 2013). In smooth muscle, the activation of G α s initiates the activation of adenylyl cyclase (AC), which converts adenosine triphosphate (ATP) into 3'-5'-cyclic adenosine monophosphate (cAMP). Inhibitory G α subunits, such as G α i/o inhibit this process. Protein kinase A (PKA) becomes active when cAMP binds, leading to release of inhibition by the PKA regulatory subunits. PKA regulates various metabolic pathways (Lee et al., 2016), cell migration (Howe, 2004), and the relaxation of airway smooth muscle (Billington et al., 2013), among other functions (Sadeghian et al., 2022; Torres-Quesada et al., 2017).

The <u>C. elegans</u> spermatheca stores sperm and is the site of fertilization. In the spermatheca, acto-myosin contractility is activated by Ca^{2+} signaling via the phospholipase <u>PLC-1</u>, which stimulates the release of Ca^{2+} from the endoplasmic reticulum. In previous work, we identified <u>GSA-1</u> (G α s) signaling through PKA as an important regulator of coordinated Ca^{2+} signaling in the spermatheca (Castaneda et al., 2020). Oocyte entry initiates a series of Ca^{2+} oscillations, which lead to contraction and the exit of the fertilized egg into the uterus. Several crucial questions remain, such as what initiates this signaling cascade and maintains these Ca^{2+} oscillations and how the combined perception of mechanical and biochemical cues leads to proper response observed at the tissue level.

Here we show that, in addition to GSA-1 (G α s), GOA-1 (G α i/o), also regulates spermathecal contractility. GOA-1 is expressed pan-neuronally where it regulates secretion of neurotransmitters impacting *C. elegans* physiology, development, behavior and egg laying (Bastiani, 2006; Ravi et al., 2021; Rose & Gönczy, 2014). To regulate egg laying, GOA-1 depresses Ca²⁺ signaling in the hermaphrodite specific neuron (HSN) (Ravi et al., 2021). A *goa-1p*::GOA-1::GFP construct is also expressed in the spermatheca and other tissues (Figure 1A). To determine if GOA-1 regulates transit of eggs through the spermatheca, fluorescent signal from the Ca²⁺ sensor GCaMP was used to visualize the spermatheca. In this experiment, the percentage of spermathecae occupied with an oocyte was determined for each gene. If the gene is required for oocyte transit through the spermatheca, the percentage of occupied spermatheca will be higher than the negative control condition. About 20% of the spermathecae were occupied by an oocyte in negative control RNAi while the positive controls (*plc-1* and *gsa-1* RNAi) show more than 95% spermathecal occupancy. Depletion of GOA-1 by RNAi, or by the loss of function (lf) allele *goa-1*(*sa734*), results in a failure of embryos to exit the spermatheca (Figure 1B). Because GOA-1 is an inhibitory G α subunit, we predicted this phenotype might be shared by animals expressing a *gsa-1* gain of function allele, *gsa-1*(*ce94*). In *gsa-1*(*gf*) animals, however, most embryos successfully exit the spermatheca (Figure 1B).

During wild type ovulations, the spermatheca exhibits stereotypical Ca^{2+} transients, which alternate in distal and proximal pulses. Distal pulses increase in intensity as the embryo exits (Kovacevic et al., 2013). To visualize the Ca^{2+} transients, GCaMP timelapse images were acquired at one frame per second and displayed as kymograms (see Methods) where the spatial dimension from distal to proximal across the spermatheca is plotted against the timepoint in the transit. In both gsa-1(gf) and goa-1(lf) spermathecae, repetitive pulses of Ca^{2+} are observed throughout the duration of the ovulation (Figure 1C-E). The gsa-1(gf) and goa-1(lf) kymograms shown are representative of those in which the embryos failed to exit the spermatheca. Both alleles are predicted to increase the activity of adenylyl cyclase, resulting in increased cAMP, activation of PKA and Ca^{2+} release (Bastiani, 2006), and we have shown previously that gsa-1(gf) results in strong pulses of Ca^{2+} in the spermatheca (Castaneda et al., 2020). In order for the embryo to exit, the contractions of the spermathecal bag need to be coordinated with relaxation of the spermathecal-uterine valve. This coordination seems to be disrupted in both gsa-1(gf) and goa-1(lf) animals.

To identify regulators and effectors of GOA-1 in the spermatheca, potentially including the GPCR, we tagged GOA-1 with the biotin ligase TurboID for proximity labeling (Branon et al., 2018; Cho et al., 2020) under the control of <code>fkh-6</code>, a spermathecal-specific promoter (Hope et al., 2003). Western blotting confirmed that GOA-1::TurboID successfully biotinylated proteins (Figure 1F). Mass spectrometry analysis was used to identify the labeled proteins. Animals expressing TurboID alone (<code>fkh-6p::TurboID</code>) and wildtype N2 animals were used as controls. We identified 16 proteins that were biotinylated specifically in triplicate GOA-1::TurboID samples. The identities and homologies of the replicated TurboID targets are shown in Table 1. The beta subunit GPB-1 was among the GOA-1::TurboID targets identified, but only in one replicate, suggesting this screen is not saturating for GOA-1 interactors in the spermatheca. We next functionally characterized the GOA-1::TurboID targets for potential roles in transit of oocytes through the spermatheca. We used the same GCaMP expressing strain for each of the 16 genes and scored occupied spermathecae. None of the 16 genes showed a significant spermathecal phenotype (Figure 1G).

Although we identified no significant spermathecal phenotype by RNAi for these 16 genes, stronger knockdown or analysis of mutant alleles may reveal a role for these genes in the spermatheca. Time-lapse GCaMP imaging may reveal more subtle effects on Ca²⁺ coordination during spermathecal transits. For example, PIEZO1/*pezo-1* does have a known spermathecal phenotype and regulates reproductive tissue contractility (Bai et al., 2020). Some of the other genes may also regulate cell contractility. For example, NATC-1 expression suggests it may be relevant to contractility regulation in



the sheath and distal tip cells (Warnhoff et al., 2014). <u>PBO-4</u> and <u>TWK-18</u> are expressed in body wall muscle and are expected to regulate muscle contraction (Beg et al., 2008; Kunkel et al., 2000). The next step is to study if these genes show phenotypes with stronger RNAi knock-down or alleles, and if so, to determine whether they interact with <u>GOA-1</u>.

Table1: Mass spectrometry results of <u>GOA-1</u> targets and human homology of the TurboID targets from WormBase and NCBI.

<u>C.</u> <u>elegans</u> genes	Functions	Human homology	Functions	
<u>alh-3</u>	aldehyde dehydrogenase (NAD+) activity and formyltetrahydrofolate dehydrogenase activity	aldh1l2	Mitochondrial 10-formyltetrahydrofola te dehydrogenase	
<u>aqp-1</u>	channel activity	aqp10	Homotetrameric transmembrane channels	
arrd-25	protein transport	arrdc2	Unknown	
<u>C07D8.6</u>	aldose reductase (NADPH) activity	akr1c4	Cytosolic aldo-keto reductase	
enol-1	phosphopyruvate hydratase activity	eno2	enolase isoenzymes	
<u>F38E9.1</u>	phosphoric diester hydrolase activity	plcxd2	Phosphatidylinositol catalysis	
natc-1	peptide alpha-N-acetyltransferase activity	naa35	N-terminal methionine acetylation catalysis	
<u>pbo-4</u>	potassium:proton antiporter activity and sodium:proton antiporter activity.	Slc9a2	Plasma membrane Na+/H+ antiporter	
<u>pes-7</u>	GTPase activator activity; actin filament binding activity; and calmodulin binding activity	iqgap2	CDC42 and RAC1 activator, associates with calmodulin	
<u>pezo-1</u>	mechanosensitive monoatomic ion channel activity and monoatomic cation channel activity	piezo2	Pore-forming mechanosensitive non- specific cation Piezo channel	
<u>r102</u> .2	Expressed in neurons.	No homology	N/A	
<u>snf-3</u>	amino-acid betaine transmembrane transporter activity	slc6a1	gamma-aminobutyric acid (GABA) transport	
<u>adh-1</u>	alcohol dehydrogenase (NAD+) activity	adh4	NAD-dependent oxidation catalysis	
<u>T21B6.3</u>	body wall musculature and muscle cell	hmcn1	growth factor beta-mediated rearrangement	
<u>twk-18</u>	rectifier potassium channel activity	kcnk18	Rectifying K+ channel	
<u>vps-26</u>	intracellular protein transport and retrograde transport, endosome to Golgi	vps26b	vesicular protein sorting	

Methods

C. elegans strains and culture



Nematodes were grown on NGM plates (0.107 M NaCl, 0.25% wt/vol Peptone, 1.7% wt/vol BD BactoAgar, 2.5 mM KPO₄, 0.5% Nystatin, 0.1 mM CaCl₂, 0.1 mM MgSO₄, 0.5% wt/vol cholesterol) and fed with *E. coli* OP50 at 23°C. All extra-chromosomal arrays of fkh-6p::TurboID (20 ng/ml), fkh-6p::TurboID (10 ng/ml), and an injection marker (50 ng/ml) were injected into N2 animals. Transgenic animals were integrated by UV radiation. Strains used are listed in Table 2.

RNA interference

The RNAi protocol was performed as described previously (Timmons & Fire, 1998). $\underline{HT115}(DE3)$ bacteria (RNAi bacteria) transformed with a dsRNA construct of interest was grown overnight in Luria Broth (LB) supplemented with 40 µg/ml ampicillin and seeded (150 µl) on NGM plates supplemented with 25 µg/ml carbenicillin and disopropylthio- β -galactoside (IPTG). Seeded plates were left for 24–72 hours at room temperature (RT) to induce dsRNA expression. Empty pPD129.36 vector ("Control RNAi") was used as a negative control in all RNAi experiments.

Embryos from gravid adults were collected using an alkaline hypochlorite solution as described previously (Hope, 1999) and washed three times in M9 buffer (22 mM KH_2PO_4 , 42 mM $NaHPO_4$, 86 mM NaCl, and 1 mM $MgSO_4$). Clean embryos were transferred to supplemented NGM plates seeded with $\underline{HT115}$ (DE3) bacteria expressing dsRNA of interest and left to grow at 23°C for 50–56 hours depending on the experiment.

Spermathecal occupancy and GCaMP imaging

To prepare age-matched young adult animals for the spermathecal occupancy and transit assays, gravid hermaphrodites were lysed in an alkaline hypochlorite solution to release eggs, which were then placed onto seeded NGM plates and grown at 23°C for 52 hours. Animals were mounted on 5% agarose in 0.1 M sodium azide and observed immediately with DIC and fluorescence microscopy to score spermathecal occupancy rates. For timelapse GCaMP imaging, animals were immobilized on 3% agarose gel with 0.05 micron polystyrene polybeads diluted 1:2 in water (Polysciences Inc., Warrington, PA, USA). Time lapse GCaMP imaging was captured automatically at 1 frame per second, with an exposure time of 20 ms and a gain of 8. All images from the timelapse were registered, rotated and oriented with the sp-ut valve on the right of the frame. An 800 x 400 pixel region of interest encompassing the entire spermatheca was selected to measure the GCaMP3 signal. The kymograms were constructed using a custom ImageJ macro as described previously. Briefly, for each frame of the movie, the pixel values in each column were averaged to collapse the image to one row. Then, each row was stacked to form the kymogram. All imaging was performed on a Nikon Eclipse 80i microscope with a 60x oil-immersion lens using SPOT Advanced software (Version 5.3.5) and the Spot RT3 CCD camera. (Castaneda et al., 2020).

Biotinylation, western blotting, and mass spectrometry

Protein lysates were prepared from age-matched fkh-6p::GOA-1::TurboID, fkh-6p::TurboID and N2 animals grown on E. $coli\ HT115(DE3)$ as follows: Animals were washed from plates using M9 and allowed to settle and then frozen at -80°C. Animals were resuspended in RIPA lysis buffer containing protease inhibitors (Sanchez & Feldman, 2021). Protein extracts were obtained by sonication at 20% at 10 s intervals for 60 s total. The protein was quantified using the BCA Protein assay. Pierce streptavidin-coated magnetic beads (125 μ l) were added to 1 mg of protein for each sample (~250 μ l), and the lysate was rotated gently at 4°C for 16 h. Then, the samples were washed multiple times with buffers as described (Sanchez & Feldman, 2021).

Samples were loaded onto Mini-PROTEAN TGX precast 10% polyacrylamide gels (Bio-Rad; Hercules, CA, USA) for SDS-PAGE. Antibodies used for Western blotting were Anti-Biotin Antibody at 1:1000 (SC-101339, Santa Cruz Biotechnology) for primary antibody, and donkey anti-mouse IgG at 1:2000 (SA1100, Thermo Scientific Pierce) for secondary antibody.

The eluted samples were sent for proteomic analysis. The proteins were briefly run in a 10% acrylamide gel to clean the samples followed by in gel reduction, alkylation and trypsin digestion (Shevchenko et al., 2006). The resulting peptides were desalted with a C18 column (Pierce), dried down and reconstituted with 0.1% formic acid. Proteomic analysis was carried on a Thermo Fisher QExactive Orbitrap in line with a Thermo Fisher RSLC Ultimate 3000 nanoUPLC. The peptides were loaded onto an in-house pulled tip 75 μm x 20 cm C18 ReproSil-Pur 120 1.9 μm (Dr. Manetsch) LC column and separated with the following gradient: buffer A; 0.1% formic acid, buffer B; acetonitrile with 0.1% formic acid, 0-25 min: 2% B, 25-145 min: 2-35% B, 145-154 min: 35-95% B, 154-159 min: 95% B, 159-160 min: 95-2% B, 160-180 min: 2% B. The flow rate was set to 200 nL/min. The settings were as follows: spray voltage 1.5 kV, sheath gas flow rate 10, capillary temperature 250°C, S-lens RF level 65. The data was acquired using a top 20 data dependent acquisition scan with the following parameters: for MS1, the resolution was set at 70,000, AGC target at 3e6, max IT 100 ms with a scan range from 350 to 1500 m/z. For MS2, the resolution was set at 17,500, the AGC target at 1e5 and the maximum IT at 100 ms with an isolation window of 1.6 m/z and a collision energy of 30. The resulting spectra were analyzed with Proteome Discoverer 3.0 with a canonical <u>C. elegans</u> FASTA file containing 4462 proteins, a common contaminant database, cysteine carbamidomethyl (+57.02 Da) set as a fixed modification, methionine oxidation (+15.99 Da) set as a dynamic modifications.



Proteins were filtered to 1% false discovery rate. A list of proteins identified by mass spectrometry in three replicates is shown in Table 1.

Image analysis and Statistics

ImageJ (FIJI) (version 2.16.0) was used for image analysis. GraphPad Prism (version 10.5.0) was used for statistical analyses. Phenotype distributions were evaluated with Fisher's exact test. In both cases, the Benjamini-Hochberg correction was applied to adjust for multiple trials.

Reagents

Table 2: Strains

Strains	Genotype	Available from
<u>UN1108</u>	xbIs1101 [<u>fln-1</u> p::GCaMP3, <u>rol-6</u>]	Cram lab
<u>UN1718</u>	xbIs1101 [<u>fln-1</u> p::GCaMP3, <u>rol-6</u>]; <u>goa-1(sa734</u>)	Cram lab
<u>UN1774</u>	xbIs1101 [<u>fln-1</u> p::GCaMP3, <u>rol-6</u>]; <u>gsa-1(ce94</u>)	Cram lab
U <u>N2</u> 301	xbIs2301 [<i>fkh-6p</i> :: <u>GOA-1</u> ::TurboID::3xHA; <i>rol-6</i>]	Cram lab
U <u>N2</u> 306	xbIs2306 [fkh6-p::TurboID::3xHA; rol-6]	Cram lab
LX2071	vsSi32 [<i>g<u>o</u>a-1</i> ::GFP + <u>unc-119(</u> +)] III	CGC

Table 3: Antibodies

Antibody	Animal and clonality	Description
Anti-Biotin	Mouse	SC-101339, Santa Cruz Biotechnology
Donkey anti- <u>mouse</u>	Donkey	SA1100, Thermo Scientific Pierce

Acknowledgements: We thank members of the Cram and Apfeld labs for helpful discussions. Undergraduate researchers, Huiyun Wang and Sanya Sharma, contributed to the RNAi screening.

References

Bai X, Bouffard J, Lord A, Brugman K, Sternberg PW, Cram EJ, Golden A. 2020. Caenorhabditis elegans PIEZO channel coordinates multiple reproductive tissues to govern ovulation. eLife 9: 10.7554/elife.53603. DOI: 10.7554/eLife.53603

Bastiani C. 2006. Heterotrimeric G proteins in C. elegans. WormBook : 10.1895/wormbook.1.75.1. DOI: doi.org/10.1895/wormbook.1.75.1

Beg AA, Ernstrom GG, Nix P, Davis MW, Jorgensen EM. 2008. Protons Act as a Transmitter for Muscle Contraction in C. elegans. Cell 132: 149-160. DOI: 10.1016/j.cell.2007.10.058

Billington CK, Ojo OO, Penn RB, Ito S. 2013. cAMP regulation of airway smooth muscle function. Pulmonary Pharmacology & Therapeutics 26: 112-120. DOI: 10.1016/j.pupt.2012.05.007

Branon TC, Bosch JA, Sanchez AD, Udeshi ND, Svinkina T, Carr SA, et al., Ting. 2018. Efficient proximity labeling in living cells and organisms with TurboID. Nature Biotechnology 36: 880-887. DOI: doi.org/10.1038/nbt.4201

Castaneda PG, Cecchetelli AD, Pettit HN, Cram EJ. 2020. Gα/GSA-1 works upstream of PKA/KIN-1 to regulate calcium signaling and contractility in the Caenorhabditis elegans spermatheca. PLOS Genetics 16: e1008644. DOI: 10.1371/journal.pgen.1008644

Cho KF, Branon TC, Udeshi ND, Myers SA, Carr SA, Ting AY. 2020. Proximity labeling in mammalian cells with TurboID and split-TurboID. Nature Protocols 15: 3971-3999. DOI: doi.org/10.1038/s41596-020-0399-0



Hope, I. A. (Ed.). 1999. *C. elegans: A Practical Approach*. Oxford University Press. https://doi.org/10.1093/oso/9780199637393.001.0001 DOI: 10.1093/oso/9780199637393.001.0001

Hope I. A., Mounsey, A., Bauer, P., & Aslam, S. 2003. The forkhead gene family of Caenorhabditis elegans. Gene 304: 43-55. DOI: doi.org/10.1016/S0378-1119(02)01175-7

Howe AK. 2004. Regulation of actin-based cell migration by cAMP/PKA. Biochimica et Biophysica Acta (BBA) - Molecular Cell Research 1692: 159-174. DOI: 10.1016/j.bbamcr.2004.03.005

Jastrzebska B. 2013. GPCR: G protein complexes—the fundamental signaling assembly. Amino Acids 45: 1303-1314. DOI: 10.1007/s00726-013-1593-y

Kovacevic I, Orozco JM, Cram EJ. 2013. Filamin and Phospholipase C-ε Are Required for Calcium Signaling in the Caenorhabditis elegans Spermatheca. PLoS Genetics 9: e1003510. DOI: <u>10.1371/journal.pgen.1003510</u>

Kunkel MT, Johnstone DB, Thomas JH, Salkoff L. 2000. Mutants of a Temperature-Sensitive Two-P Domain Potassium Channel. The Journal of Neuroscience 20: 7517-7524. DOI: 10.1523/JNEUROSCI.20-20-07517.2000

Lee JH, Han JS, Kong J, Ji Y, Lv X, Lee J, Li P, Kim JB. 2016. Protein Kinase A Subunit Balance Regulates Lipid Metabolism in Caenorhabditis elegans and Mammalian Adipocytes. Journal of Biological Chemistry 291: 20315-20328. DOI: 10.1074/jbc.M116.740464

Ravi B, Zhao J, Chaudhry SI, Signorelli R, Bartole M, Kopchock RJ, et al., Collins. 2021. Presynaptic Gαo (GOA-1) signals to depress command neuron excitability and allow stretch-dependent modulation of egg laying in *Caenorhabditis elegans*. Genetics 218: 10.1093/genetics/iyab080. DOI: 10.1093/genetics/iyab080

Rose L, Gonczy P. 2014. Polarity establishment, asymmetric division and segregation of fate determinants in early *C. elegans* embryos. WormBook: 1-43. *WormBook*: *The Online Review of C. elegans Biology*. https://doi.org/10.1895/wormbook.1.30.2 DOI: 10.1895/wormbook.1.30.2

Sadeghian F, Castaneda PG, Amin MR, Cram EJ. 2022. Functional Insights into Protein Kinase A (PKA) Signaling from C. elegans. Life 12: 1878. DOI: 10.3390/life12111878

Sanchez AD, Feldman JL. 2021. A proximity labeling protocol to probe proximity interactions in C. elegans. STAR Protocols 2: 100986. DOI: 10.1016/j.xpro.2021.100986

Shevchenko A, Tomas H, Havli J, Olsen JV, Mann M. 2006. In-gel digestion for mass spectrometric characterization of proteins and proteomes. Nature Protocols 1: 2856-2860. DOI: <u>10.1038/nprot.2006.468</u>

Timmons L, Fire A. 1998. Specific interference by ingested dsRNA. Nature 395: 854-854. https://doi.org/10.1038/27579 DOI: 10.1038/27579

Torres-Quesada O, Mayrhofer JE, Stefan E. 2017. The many faces of compartmentalized PKA signalosomes. Cellular Signalling 37: 1-11. DOI: <u>10.1016/j.cellsig.2017.05.012</u>

Warnhoff K, Murphy JT, Kumar S, Schneider DL, Peterson M, Hsu S, et al., Kornfeld. 2014. The DAF-16 FOXO Transcription Factor Regulates natc-1 to Modulate Stress Resistance in Caenorhabditis elegans, Linking Insulin/IGF-1 Signaling to Protein N-Terminal Acetylation. PLoS Genetics 10: e1004703. DOI: 10.1371/journal.pgen.1004703

Funding: Some strains were provided by the CGC, which is funded by NIH Office of Research Infrastructure Programs (P40 OD010440). This work was supported by a grant from the National Institutes of Health National Institute of General Medical Sciences (GM110268) to EC.

Author Contributions: Fereshteh Sadeghian: formal analysis, investigation, methodology, writing - original draft. Virginie Sjoelund: formal analysis, investigation, methodology. Erin J. Cram: formal analysis, funding acquisition, writing - review editing.

Reviewed By: Anonymous

Nomenclature Validated By: Anonymous WormBase Paper ID: WBPaper00068778

History: Received September 30, 2025 **Revision Received** November 3, 2025 **Accepted** November 8, 2025 **Published Online** November 10, 2025 **Indexed** November 24, 2025

Copyright: © 2025 by the authors. This is an open-access article distributed under the terms of the Creative Commons Attribution 4.0 International (CC BY 4.0) License, which permits unrestricted use, distribution, and reproduction in any medium, provided the original author and source are credited.

Citation: Sadeghian F, Sjoelund V, Cram EJ. 2025. GOA-1 regulates spermathecal transits. microPublication Biology. 10.17912/micropub.biology.001877